ELSEVIER

Nuclear Instruments and Methods in Physics Research B 157 (1999) 226–232

NIM B
Beam Interactions with Materials & Atoms

www.elsevier.nl/locate/nimb

Shallow implantation of Ti^+ ions in sapphire [α-Al_2O_3(0 0 0 1)]

H. Lee, S.M. Lee, E.T. Ada, B. Kim, M. Weiss, S.S. Perry, J.W. Rabalais *

Department of Chemistry, University of Houston, Houston, TX 77204-2641, USA

Abstract

Sapphire single crystal [α-Al_2O_3(0 0 0 1)] samples were treated by irradiation with Ti^+ ions in the energy range 0.5–7.0 keV at 25°C and 750°C under UHV conditions for total doses of 10^{16} Ti^+/cm^2. These Ti treated sapphire samples were studied by ex situ X-ray photoelectron spectroscopy (XPS) depth profiling and by atomic force microscopy (AFM). Aluminum in the oxidation states $Al^{0,3+,x+}$, where $0 < x < 3$, and titanium in the oxidation states $Ti^{0,2+,3+,4+}$ were found to coexist throughout the implanted region, with variation of their relative amounts along the depth distribution. The AFM measurements showed that there was minimal change in surface morphology following implantation at all conditions, indicating that the sapphire surface has enough resiliency to retain its original surface morphology despite the keV ion impacts.

PACS: 81.15; 68.55; 81.15.A; 81.15.H
Keywords: Deposition methods; Ion beams; Growth; Thin films; Structure

1. Introduction

The effects of ion implantation on the surface of ceramic materials has been studied extensively [1,2]. Depending on the type of ion and implantation conditions, such as incident ion kinetic energy, ion dose, and substrate temperature, effects such as amorphization, lattice deformation, phase transformation, creation of defects, and formation of fine particles of the implanted species have been observed [3–11]. Several studies have shown that ion implantation can improve the mechanical properties of sapphire, i.e. harden the near surface region and increase the fracture toughness of the material [12].

Chemical reactions between Ti and Al_2O_3 are of particular interest for the production of metal–ceramic composite materials and microelectronic packaging materials that require joining metals to ceramics [13]. Ti is often used in metal–ceramic junction processes. The chemical reactions at the interface between metals and ceramics are important for the enhancement of adhesion and long-term stability of the metal–ceramic systems. Improvements in metal–ceramic bonding might be achievable by means of pretreatment modification of the ceramic substrate surface before the joining process. The properties of the metal–ceramic bond depend on the morphology of the initial ceramic surface and the chemical states at the interface.

* Corresponding author. Tel.: +1-713-743-3282; fax: +1-713-743-2709; e-mail: rabalais@uh.edu

0168-583X/99/$ – see front matter
PII: S0168-583X(99)00438-3

Shallow implantation of low energy ions may provide the desirable pretreatment effects rather than high energy ions because the modified layers are confined to the near-surface region with low energy ions. Therefore, understanding the chemical states and morphology in the surface or near-surface region that has been modified by low energy ions is important for the development of pretreatment strategies. In this paper, the results of a study of low keV Ti^+ ions implanted into the surface and near-surface region of sapphire [α-Al_2O_3(0 0 0 1)] using X-ray photoelectron spectroscopy (XPS) depth profiling and atomic force microscopy (AFM) for analysis are presented.

2. Experimental methods

Polished single crystal sapphire [α-Al_2O_3(0 0 0 1)] samples (10×10 mm) were cleaned for 10 min with trichloroethylene and then for another 10 min with distilled water in an ultrasonic bath. The samples were introduced into the UHV chamber at 7×10^{-10} mbar and annealed at 1100°C for 1 h for further cleaning. The instrument [14] used in this shallow implantation experiment was designed specifically for low energy ion beam deposition and implantation. It provides low kinetic energy (5 eV–10 keV), mass-selected ion beams with an energy spread of ~3 eV. The incident kinetic energies of the Ti^+ ions used in this implantation were 0.5, 4, and 7 keV. The Ti^+ ion flux was measured by means of a Faraday cup mounted on the sample holder. The total dose used in each implantation was 10^{16} Ti^+ ions/cm^2. The implantation temperature was controlled by a resistively heated filament mounted behind the sample. Ti^+ ion implantation was performed at either room temperature, i.e. 25°C, or 750°C.

Ex situ XPS spectra and depth profiles were obtained for the implanted samples using a Physical Electronics Model 5700 spectrometer equipped with an Al K_α X-ray source, electron and ion beam charge compensation of the sample, and a 5 keV Ar^+ sputter source. During the XPS analysis, the samples were simultaneously irradiated by low energy (2 eV) electron and low energy (5 eV) Ar^+ ion beams. The electron flood gun compensates for the removal of electrons while the ion beam alleviates static charge build up in and around the analyzed region [21]. Atomic force microscopy (AFM) was used in the contact mode under ambient conditions to observe the surface morphology changes following implantation.

3. Results and discussion

Examples of Ti 2p and Al 2p XPS spectra of 7 keV Ti^+ implanted α-Al_2O_3(0 0 0 1) plotted at each sputter cycle interval along with an example of their deconvolution are shown in Fig. 1. Aluminum in the oxidation states $Al^{0,3+,x+}$, where $0<x<3$, and titanium in the oxidation states $Ti^{0,2+,3+,4+}$ were observed to coexist throughout the implanted region. Note that reduced Ti and Al states are observed near the surface and only highly oxidized Ti and Al states are observed near the interface. Deconvolution of the spectra was achieved by fitting the peaks with a combination Gaussian/Lorentzian peak shape following a Shirley background correction, with the variation in the peak full-width-at-half-maximum (FWHM), position, and height being determined by an iterative program. The O 1s peak position was used as a binding energy reference. Contaminant carbon and oxygen formed on the sample surface during air transfer to the XPS chamber was confined to the topmost layer and was eliminated after the first sputter cycle of the XPS depth profile. Therefore, the effect of the minimal air exposure before the ex-situ XPS measurements on the overall depth profiles was considered negligible.

Sputter depth profiling using keV Ar^+ ions has been shown to induce changes in the oxidation states of the metal atoms in metal oxides. This is often due to the preferential sputtering of O atoms [18]. Thus, it is possible that the observed reduced oxidation states of Ti and Al are due to the effects of keV Ar^+ ions during sputter depth profiling. However, since all of the Ti-implanted sapphire samples were subjected to the same depth profiling conditions, comparative analysis of the effects of the Ti^+ energy and temperature on the depth-composition profile is valid. For example, a clear effect of the incident Ti^+ ion energy is the

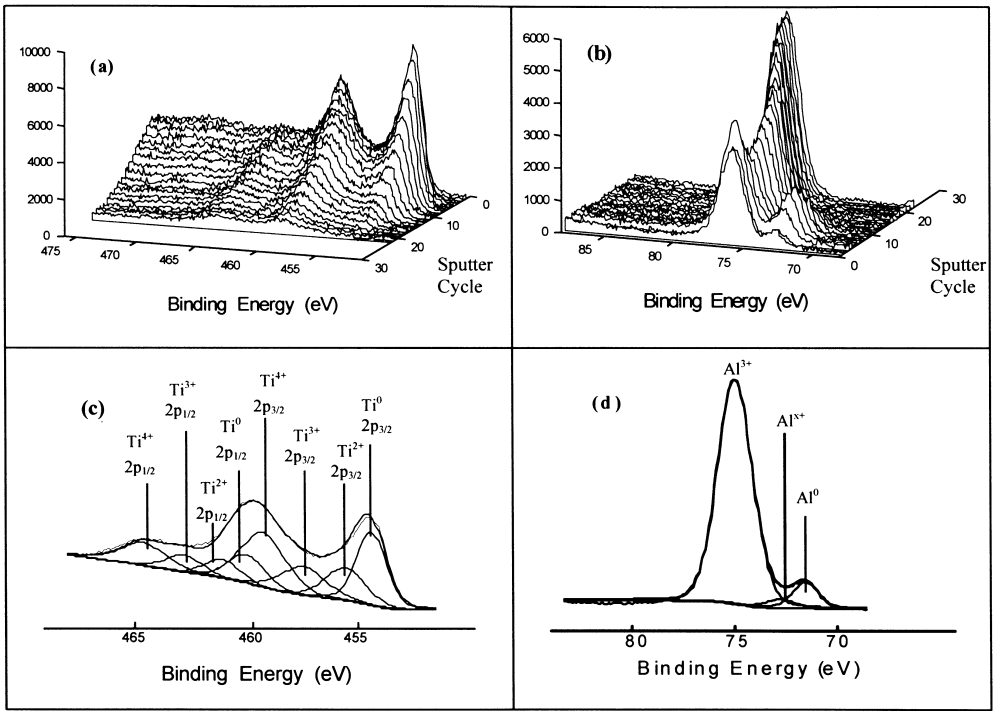

Fig. 1. Ti 2p (a) and Al 2p (b) XPS spectra as a function of Ar^+ sputtering dose for Ti^+ implanted sapphire samples. Note that the sputter cycle axes are reversed in (a) and (b) in order to more clearly show the features. Examples of deconvolutions of the Ti 2p (c) and Al 2p (d) XPS spectra. All of the spectra are for the sample implanted with 7 keV Ti^+ ions at room temperature.

formation of metallic Al states at 4 and 7 keV ion energies. The sapphire samples exposed to 0.5 keV Ti^+ ions were not found to contain metallic Al in the modified layer. If the formation of the reduced Al was due to the keV Ar^+ ions used in XPS depth profiling, it can be expected that metallic Al would be found for all three incident ion energies studied.

Fig. 1(c) shows a representative Ti $2p_{1/2,3/2}$ spectrum fitted satisfactorily with four different oxidation states of Ti. The binding energy values and the relative $2p_{1/2}$ to $2p_{3/2}$ peak area ratio (0.45) for these different oxidation states were obtained from previously published results [18,19]. These values for the Ti $2p_{3/2}$ and $2p_{1/2}$ peaks are 454.1 and 460.2 eV for Ti^0, 454.9 and 460.8 eV for Ti^{2+}, 456.9 and 462.6 eV for Ti^{3+}, and 458.9 and 464.6 eV for Ti^{4+}. For all incident ion energies and implantation temperatures studied, metallic Ti states were found to be largely present only in the near surface region while increasingly oxidized states dominate the interior of the modified layer (Fig. 1(a)). The presence of suboxides of Ti and partially reduced Al at the interface between ultrathin films of Ti metal and sapphire (0 0 0 1) has been reported earlier [22].

In the deconvolution of the Al 2p spectrum of the sample implanted with 7 keV Ti^+ at room temperature in Fig. 1(d), the appearance of two distinct peaks indicates the presence of metallic and oxidized aluminum, but attempts at deconvolution of the spectrum into two components of Al^0 and Al^{3+} were unsatisfactory. Inclusion of an additional component of intermediate oxidation state, i.e. Al^{x+}, provided the best fit to the experimental spectrum. Therefore, the XPS spectrum indicates that aluminum in the irradiated region exists in three different oxidation states, i.e. Al^0, Al^{3+}, and Al^{x+}, where $0 < x < 3$. The presence of such intermediate Al oxidation states has also been suggested in a previous study of Ti-implanted

sapphire [17]. The separation between the Al^0 and Al^{3+} peaks of ~3.4 eV is somewhat larger than the reported literature value [15,16] of ~3 eV. This larger separation value is attributed to differential charging along the depth towards the bulk sapphire.

Fig. 2 shows the depth–composition profiles for the Ti^+ implanted sapphire samples as a function of the incident ion energy and implantation temperature. The expected deeper implantation profiles for Ti with respect to the incident ion energy were observed, i.e. the maxima and the widths of the Ti profiles were progressively deeper and wider, respectively, for increasingly higher ion energies. Another evident ion energy effect is the formation of reduced Al states at high ion energies, i.e. 4 and 7 keV, and their absence at 0.5 keV. It is reasonable to suggest that O atom preferential sputtering at the higher energies is the dominant origin of this ion energy dependence of the formation of reduced Al states in the modified layer. However, TRIM calculations show that although the sputtering yields increase over the 0.5–7.0 keV range, the O/Al sputtering yield ratios are 1.51 ± 0.05, i.e. the sputtering yield ratios are constant and equal to the stoichiometric ratio of the elements in Al_2O_3. This suggests that preferential sputtering of O atoms is insignificant in this system. Despite the observation of oxidized Ti states near the interface of the Ti layer and sapphire at 0.5 keV, no detectable amounts of reduced Al^0 states were found. This is in contrast to the results of Bernath et al. [22] who found that thermal Ti atoms evaporated on sapphire induced the reduction of Al^{3+} to a metallic state. As noted earlier, the contaminant carbon and oxygen were removed during the first sputter cycle. From Fig. 2 it is seen that the total amount of Al for the 0.5 keV sample is decreasing near the surface, while for the higher energy samples the total amount of Al remains approximately constant. This decrease in the total amount of Al near the surface may be

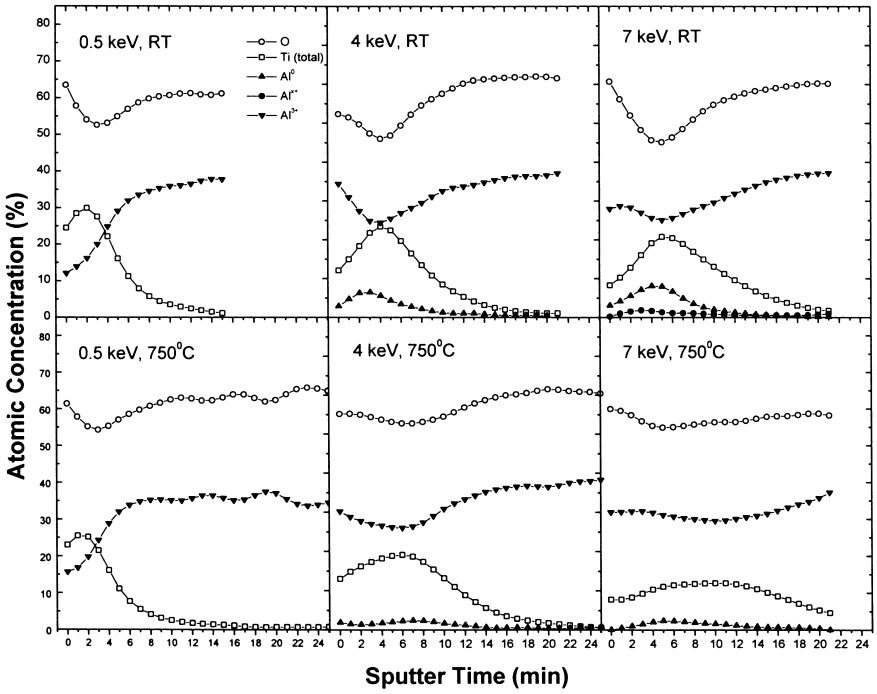

Fig. 2. XPS depth profiles of oxygen, total titanium, and aluminum in the different oxidation states, Al^0, Al^{x+}, and Al^{3+}, as a function of Ar^+ sputtering dose. The caption at the upper left corner in each depth profile indicates ion kinetic energy and temperature during the implantation.

due to a dilution effect, i.e. the implanted Ti is concentrated very near the surface resulting in dilution of the Al concentration.

The observation of $Al^{0,x+,3+}$ and $Ti^{0,2+,3+,4+}$ oxidation states along the implantation profile indicates that chemical reactions are occurring between the incoming Ti^+ ions and the Al_2O_3 lattice. The incident Ti^+ ions reduce some of the Al^{3+} in α-Al_2O_3 to Al^0 or Al^{x+}, while the Ti^+ ions themselves are oxidized to $Ti^{2+,3+,4+}$ or reduced to Ti^0. It is interesting to note that although Ti atoms in the four oxidation states $Ti^{0,2+,3+,4+}$ were found to coexist throughout the shallow implanted region with variations in their relative amounts along the depth distribution, no evidence for Ti^+ was found at any depth. This is not withstanding the fact that only Ti^+ ions were implanted into the samples and the formation of Ti_2O, in which the Ti oxidation state would be +1, was possible. While Ti^{2+} and Ti^{3+} most likely exist in their standard oxidized forms, i.e. TiO and Ti_2O_3, respectively, Ti^{4+} can be in the form of either TiO_2 or Al_2TiO_5. The latter mixed metal oxide compound is known to be formed in solid-state reactions between Al_2O_3 and TiO_2 [20]. The presence of Ti^{3+} presents the possibility that some of the incident Ti^+ ions replace Al^{3+} in an octahedral site in the Al_2O_3 hcp structure during implantation.

The metallic Ti^0 and Al^0 atoms can also exist either in the form of minute pure metal particles or in an alloy state. Since Al and Ti have similar electronegativities on the Pauling scale, an Al–Ti metallic bond is feasible. The formation of minute metallic particles has been observed for a sapphire sample implanted with a dose of $>10^{16}$ ions/cm^2 Au^+ and Fe^+ ions at 85 keV [10]. The existence of

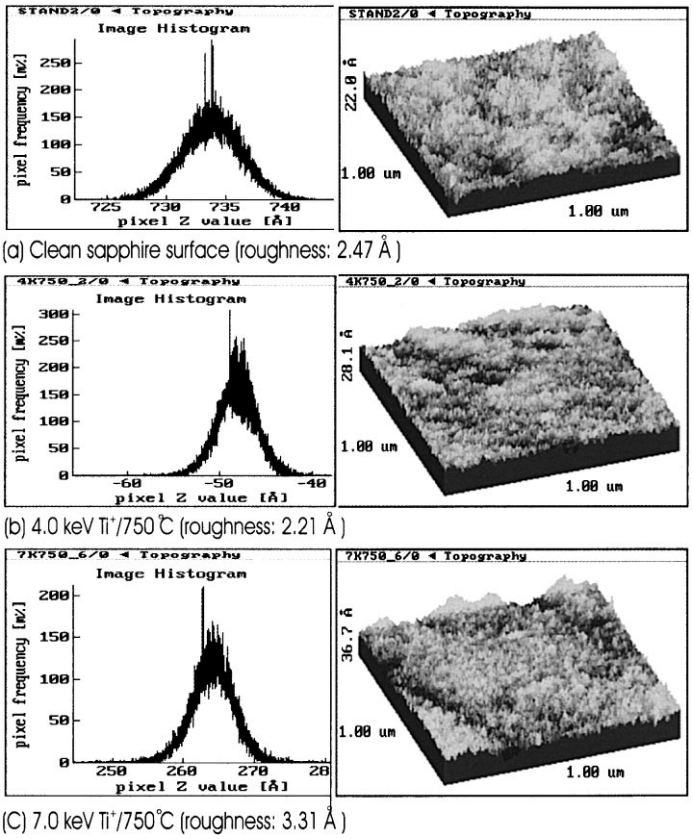

Fig. 3. AFM images of the clean sapphire surface (a) and the Ti-implanted sapphire surfaces for different energies at 750°C (b) and (c).

Al^{x+} most likely results from the formation of a mixed, nonstoichiometric bonding environment involving Al, O, and Ti, i.e. $Al_xTi_yO_z$.

Fig. 2 also shows the effects of implantation temperature on the depth-composition profiles. Significant broadening of the Ti layers was found for the 4 and 7 keV incident ion energies while almost no broadening was observed for the 0.5 keV ion energy. This suggests that at high energy implantation, diffusion of Ti atoms into the bulk is an enhanced possibility due to the greater number of defects in the sapphire. Another temperature effect is the decrease in the amount of reduced Al in the modified layer at high temperature for the 4 and 7 keV implantation. This is possibly due to two factors. First, the relatively high vapor pressure of metallic Al (10^{-5} Torr at 724°C) results in a higher desorption rate of metallic Al for the 750°C implantation. A similar mechanism has been suggested for the temperature dependence of metallic Al formation in pulsed laser deposition of α-Al_2O_3 on Si substrates [16]. Second, both the diffusion rates and the reaction probabilities of Al and O are higher at the higher temperature.

Fig. 3 shows the surface morphology and roughness values of the samples obtained by AFM before and after Ti^+ implantation. The AFM image of the clean Al_2O_3 surface is featureless, with differences in the minimum and maximum heights of only a few Angstroms. Such featureless images are observed for all of the Ti^+ irradiated samples at all energy and temperature conditions. There is no difference between the roughness values before and after implantation. The histograms of the distribution of heights are also similar for both the clean and irradiated samples. It is clear that despite the fact that chemical reactions occurred between the incident Ti^+ ions and the Al and O atoms in the sapphire, there was minimal change in the surface morphology. This indicates that the surface has sufficient resiliency to retain its original morphology, even under the impact of low keV Ti^+ ions.

4. Summary

XPS depth profiles of Ti^+ implanted sapphire samples showed the formation of aluminum in the oxidation states $Al^{0,x+,3+}$ where $0 < x < 3$. The metallic Al was observed mainly at the higher implantation energies. Even though only Ti^+ ions were implanted, titanium atoms in the oxidation states $Ti^{0,2+,3+,4+}$ were found to coexist throughout the implanted region, with variations in their relative amounts along the depth distribution. The AFM measurements showed that there was no observable change in the surface morphology after exposure to the Ti^+ ions, indicating that the sapphire surface has enough resiliency to retain its original morphology despite the keV ion impacts.

Acknowledgements

This material is based on work supported by the National Science Foundation under Grant no. DMR-9224377 and in part by the MRSEC Program of the National Science Foundation under Award no. DMR-9632667.

References

[1] J.D. Demaree, S.R. Kirkpatrick, A.R. Kirkpatrick, J.K. Hirvonen, Nucl. Instr. and Meth. B 127/128 (1997) 603.
[2] J. Bigarre, S. Fayeulle, D. Treheux, J. Appl. Phys. 82 (1997) 3740.
[3] P.J. Burnett, T.F. Page, Radiat. Eff. 97 (1986) 123.
[4] C.J. MacHargue, R. Kossowsky, W.O. Hofer, Structure–Property Relationships in Surface Modified Ceramics, NATO ASI Series, Kluwer Academic Publishers, Dordrecht, 1989, p. 253.
[5] C.J. MacHargue, P.S. Sklad, C.W. White, Nucl. Instr. and Meth. B 46 (1990) 79.
[6] C.W. White, C.J. MacHargue, P.S. Sklad, L.A. Boatner, G.C. Farlow, Mater. Sci. Rep. 4 (1989) 41.
[7] N. Moncoffre, Nucl. Instr. and Meth. B 59/60 (1991) 1129.
[8] S.J. Zinkle, Nucl. Instr. and Meth. B 91 (1994) 234.
[9] S.J. Zinkle, J. Nucl. Mater. 219 (1995) 113.
[10] T. Kobayashi, A. Nakanishi, K. Fukumura, G. Langouche, J. Appl. Phys. 83 (1998) 4631.
[11] H. Abe, S. Yamamoto, H. Naramoto, Nucl. Instr. and Meth. B 127/128 (1997) 170.
[12] C.J. MacHargue, W.B. Snyder, Jr., Passive materials for optical elements II, Proc. SPIE (1993) 135.
[13] S.F. Ohuchi, M. Kohyama, J. Am. Ceram. Soc. 74 (1991) 1163.
[14] A.H. Al-Bayati, D. Marton, S.S. Todorov, K.J. Boyd, J.W. Rabalais, D.G. Armour, J.S. Gordon, G. Duller, Rev. Sci. Instr. 65 (1994) 2680.

[15] F. Silvain, T. Carney, Thin Solid Films 330 (1998) 132.
[16] B. Hirschauer, S. Soderholm, G. Chiaia, U.O. Karlsson, Thin Solid Films 305 (1997) 243.
[17] J.H. Selverian, F.S. Ohuchi, M. Bortz, M.R. Notis, J. Mater. Sci. 26 (1991) 6300.
[18] K.J. Kim, D.W. Moon, S.H. Nam, W.J. Lee, H.G. Kim, Surf. Inter. Anal. 23 (1995) 851.
[19] K. Tamura, U. Bardi, Y. Nihei, Surf. Sci. 197 (1988) L281.
[20] E. Kato, K. Daimon, J. Takahashi, J. Am. Ceram. Soc. 63 (1980) 355.
[21] P.A.W. van der Heide, J.W. Rabalais, Chem. Phys. Lett. 297 (1997) 350.
[22] S. Bernath, T. Wagner, S. Hofman, M. Ruhle, Surf. Sci. 400 (1998) 335.